RESEARCH ARTICLE

Sheath Bone Formation and Biomechanics on Dental Implant

Haruyuki Kawahara

Emeritus Professor, Osaka Dental University, Guest Professor, Asahi University, Dental School
Director, Institute of Clinical Materials, Osaka, Japan

Correspondence: Haruyuki Kawahara, 1-22-27, Tokocho, Moriguchi, Osaka 570-0035, Japan, Phone: +81-6-6993-1011 Fax: +81-6-6993-3311, e-mail: office@icm.ac

ABSTRACT

Quick reconstruction is a trendy theme in oral implantology, especially in esthetic area. It is important how to build up rapidly and keep reliable fixation of implant in the case of immediate placement and loading after tooth extraction. This review paper is devoted to explain generation and growth of the sheath bone keeping the implant fixation under functional mastication, from biomechanical data of animal experiments.

Bone tissue may examine implant materials and conclude that they are foreign body, and responds to them as foreign objects to be attached and digested. If this is impossible, the implant materials are walled off with fibrous tissue layer, changes lately to bone tissue that is the sheath bone. This healing process after implantation into bone tissue is similar to that of soft tissue. The first step is encapsulation with fibrous layer around the implant, 1 to 2 weeks postimplantation. At the second step, the fibrous capsule changes to pseudo-bone of solution medicated calcification layer on which woven bone of primary sheath bone originates and grows, 2 weeks (6 weeks in human) postimplantation. At the third step, the primary sheath bone is developed and changed to mature sheath bone by lamellar bone compaction and apposition, 6 weeks (24 weeks in human) postimplantation. The sheath bone generation is not an exclusive reaction to specific implant biomaterials, but only expression of a nonspecific and basic healing potential in bone. The implant can develop the healing process with osteogenesis and osseointegration at the implant/bone interface even under the condition of immediate loading, when the implant is controlled within ≤ 50 µm of micromotion. The 50 µm of micromotion was recognized from relationship between implant's displacement and Periotest® value PTV, and could be maintained in the case of implant fixed with healthy cortical bone and/or connected to approximal tooth. If the implant was controlled within 50 µm of micromotion under the functional biting, the histological observations demonstrated that the implant was supported with the biodynamic interface, which represented the both status of superior bone formation and inferior bone resorption, but not supported with inferior bone formation.

1. How to control the micromotion? 2. How to read the micromotion numerically? 3. How to evade biting stress for the sheath bone formation? It has been revealed that the sheath bone requires one or more of following four conditions to resist functional biting stress until 4 months (6 months in humans) after the implantation:

1. Sufficient anchor between implants and cortical bone
2. Implant fixation with metallic stent on alveolar bone
3. Fixation by connection to approximal steady implant and/or healthy tooth
4. No load bearing condition (submersible implant).

Bone resorption and formation should be observed constantly in alveolar bone under the functional biting stress at the implant/bone interface and controlled with minimum effective strain of MES 1000 µε below (remodeling) and above (resorption). If the implant is supported with the sheath bone of less than 1000 µε under the functional mastication, the implant can keep the reliable fixation in alveolar bone. The implant/bone interface has a biodynamic interface with turnover phenomenon, bone resorption and formation by remodeling cycle with 12 weeks interval (18 weeks in humans). The healthy condition of implant has to be kept by self healing behavior of the remodeling cycle for 10 years or more. It is difficult to investigate the true nature of long-term interactions at the implant/bone interface under functional condition from the data of pinpoint observations on limited area and time by light and electron microscopy. It is important to collate the both data from basic research and clinical investigations with long-term throughout the implant life. Further studies on the bone response to biodynamic interface should be needed to enhance the reliability of dental implant fixation.

Keywords: Implant sheath bone formation, Loading, Biomechanics.

INTRODUCTION

In relation to clinical investigation on implant materials and surgery, FDI/ISO-recommendation for biological standardization of biomaterials have furnished a useful suggestion of three levels of biological testing, initial tests of tissue culture (*in vitro*), secondary tests of animal experiment (*in vivo*) and usage tests of animal experiment (with clinical condition). There is, however, no literature which shows that a good correlation exists between the tests at various levels and which would make it possible to replace a screening test at the usage level.[1,2] Therefore, clinical investigation should be considered from the experimental results of the three levels to have the final judgment on quality of implant materials and surgical procedures. Of course, the clinical investigation should be strictly controlled with biostatistic analysis on digital data from symptoms in

each patient of individual with macro size of meter unit, in which the data are frequently different from that of basic investigations, *in vitro* as well as *in vivo* examinations with micro/nano-size.[3,4]

In this paper, the growth and mechanical strength of sheath bone surrounding implant fixture will be discussed regarding the relevancy between clinical data and basic investigations on osteogenesis and osseointegration *in vivo*.

SHEATH BONE FORMATION AS A RESULT OF FOREIGN BODY REACTION

Biocompatibility of materials is defined in terms of nontoxicity, nonirritability, nonallergenicity and noncarcinogenicity including bioactive and bioreactive phenomena. In soft tissue, the biocompatible materials (biomaterials) are encapsulated with fibrous tissue a few weeks after implantation to isolate it from the host tissue as a foreign body. On the fibrous capsule, Ratner hypothesized that nonspecifically adsorbed protein films to the biomaterials are similar among most biomaterials that lead to similar healing process in soft tissue. Importantly, there is no parallel to this type of non-specific protein surface to the host tissue. The host tissue may examine such protein films, conclude they are foreign body and respond to them as foreign objects to be attached and digested.[5] If this is impossible, the biomaterials are walled off with fibrous tissue layer in soft tissue as well as with bone tissue layer in bone. The growth of primary sheath bone is scheduled as follows (Fig. 1):

1. First stage, 0 to 2 weeks postimplantation: A hematogenic stem cells (HSC) layer consisting of neutrophils, monocytes, macrophages and giant cells cover the biomaterials surface as a foreign body (red line 1, Fig. 1).
2. Second stage, 2 to 6 weeks postimplantation: Osteogenic stem cells migrate onto the HSC layer, forming collagen fiber capsulation and produce woven bone of primary sheath bone (red line 2, Fig 1).
3. Third stage, 6 to 24 weeks postimplantation: Lamellar bone apposition and compaction to woven bone change the primary sheath bone to mature sheath bone (red line 3, Fig 1). Finally, the indigestible biomaterials are encapsulated completely with the sheath bone as a foreign body in bone tissue.

Healing process after implantation in bone tissue is similar to that in soft tissue. The first step is capsulation with fibrous layer around the implant. At the second step, the fibrous capsule changes to pseudo bone on which woven bone originates and develops, successively the sheath bone is completed with maturation by lamellar bone apposition. The sheath bone generation is not an exclusive reaction to specific biomaterials, that is only an expression of a non-specific and basic healing potential of bone (Figs 2 and 3).

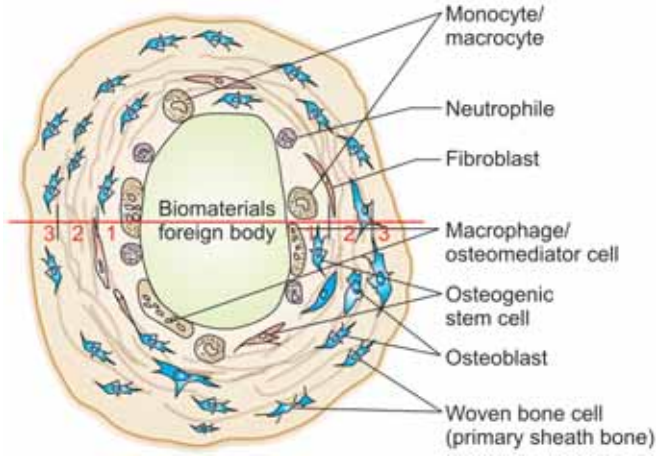

Fig. 1: Schema of time schedule on sheath bone growth

SHEATH BONE FORMATION OF TITANIUM IMPLANT

Animal Examination

Dental implants have been utilized commonly for aged patients, so the mechanism of sheath bone formation should be investigated with examination using aged animals. Rod type one piece implants of 2 mm diameter and 12 mm length were made of commercially pure titanium to investigate the sheath bone formation. The root parts have two types of surface roughness, small roughness (SR, Ra 0.4 ± 0.01 µm) and large roughness (LR, Ra 2.0 ± 0.12 µm). Eight implants each of SR and LR were implanted into jaw bones, 6 months

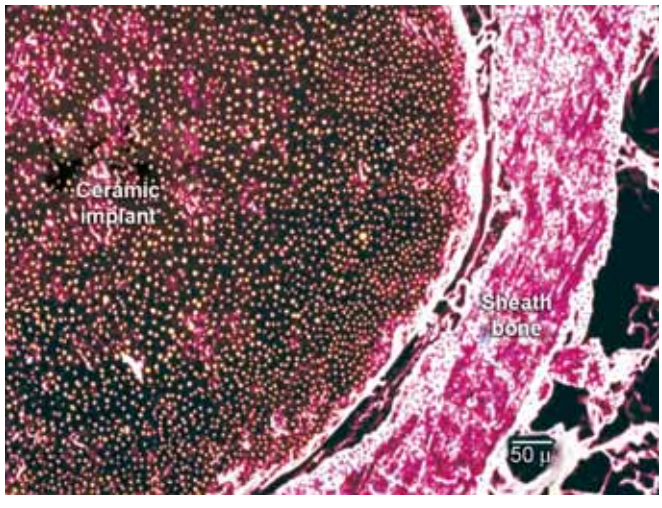

Fig. 2: Sheath bone surrounding ceramic implant 12 weeks post implantation in dogs mandible. Yellow spots: alumina, blue spots: phosphorus, red spots: calcium. Interspace between implant and sheath bone is artifact caused by tissue shrinkage

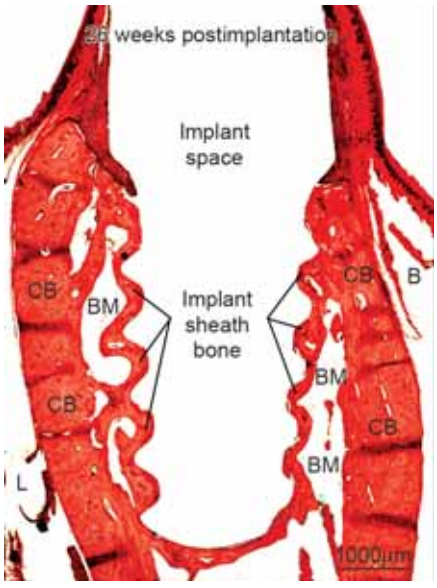

Fig. 3: Sheath bone growth in monkey's (*Macaca fascicularis*) mandible covers whole surface of implant. L: lingual side, B: buccal side, BM: bone marrow, CB: cortical bone *(courtesy: Dr T Sugimoto)*.

after extraction of P_3 and P_4 in aged beagles of 6 to 7 years old (equivalent to aged implant patients). The implants were combined to the proximal teeth P_2 and M_1 with hard resin bridge one week postimplantation. Provisional hard resin bridge was replaced with metal bridge made of Au-Pd-Ag alloy three weeks postimplantation to protect micromotion of the implants under functional biting load (Fig. 4).[6,7] We recommend 40 to 50 mm grinding off the working surface of implant crown opposing to natural tooth by checking with articulating strip to eliminate biting impact. One, four and six months postimplantation, electron microscopic observation on the process of sheath bone formation was investigated with nondecalcified specimens.

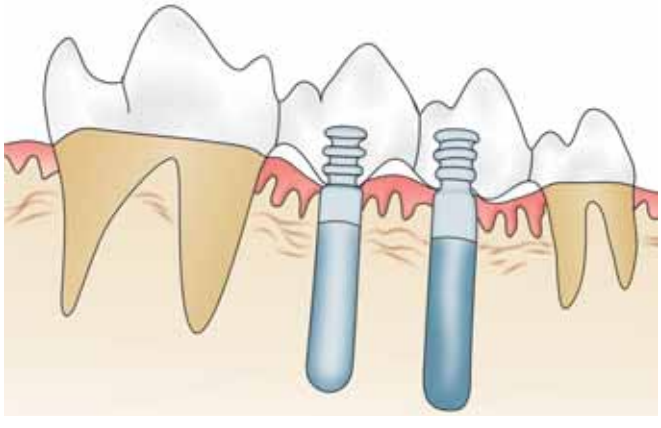

Fig. 4: Two rod-type titanium implants combined to the proximal teeth of M_1 and P_2 with metallic bridge made of Au-Pd-Ag alloy. Left implant: small roughness (SR), Ra = 0.4 ± 0.01µm, Rz = 2.9 ± 0.16 µm, Rmax = 3.6 ± 0.36 µm, Sm = 2.9 ± 0.3 µm; Right implant large roughness (LR), Ra = 2.00.12 µm, Rz = 11.2 ± 0.58 µm, Rmax = 29.1 ± 8.6 µm, Sm = 39.2 ± 9.1 µm

Growth of Sheath Bone

The implant was placed into a bone marrow throughout cortical bone layer. Primary implant stability was achieved mainly by anchoring with cortical bone, because bone marrow demonstrated less than 35% of trabecular bone density in the aged dogs similar to human alveolar bone, have 37.9 ± 4.0% in male, 32.6 ± 3.6% in female, 20 to 75 years old Japanese (Figs 5A and B).[8]

At the most early stage of five days implantation, the implant surface was covered by blood coagulation with hematogenic stem cells (HSC) including phagocytic monocytes that possessed pluripotential for the cell-differentation, e.g. to macrophage, osteoclast and osteomediator cell (OMC).[9] Osteogenic stem cells (OSC) of endosteum migrated to the implant surface from endosteal surface of cortical bone and produced multiple cell-layer on the implant surface three weeks postimplantation (Figs 6A to C). The multiple cell-layer of 25 to 150 µm thickness was constructed with HSC adhered to implant surface and OSC migrated from the endosteum. Woven bone formation at the implant surface was performed mainly by migration of OSC from the endosteum of alveolar cortical bone rather than the adjacent trabecular bone, especially in the case of yellow marrow. The OSC migration from the endosteum to the implant surface was considered as a main factor to dominate the woven bone formation at the implant surface (Figs 7A and B).[7]

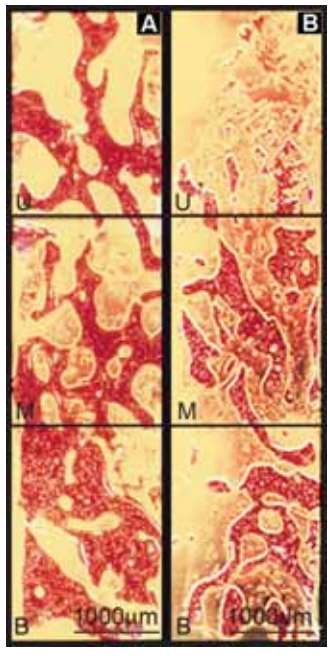

Figs 5A and B: Trabecular bone density (%) in alveolar bone marrow, (A) U: upside near crestal 33%, M: medium 48%, B: bottom 59%, average 41%, region 24, 58 years old male using partial denture for 5 years. (B) U: 14%, M: 27%, B: 29%; average 23%, region 46, 64 years old male wearing metallic bridge for 8 years *(courtesy: Dr T Nakamura)*

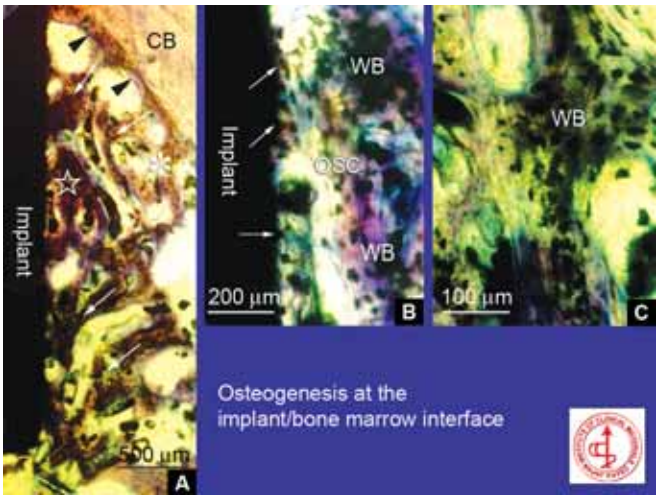

Figs 6A to C: (A) Active migration of osteogenic stem cells OSC (white arrow) from endosteum (arrow head) of cortical bone CB to the implant surface, three weeks postimplantation of SR (small roughness, Ra 0.4 µm). (B) Large magnification at star marked in (A). OSC migration covers hematogenic stem cells HSC layer adhered to the implant surface prior (white arrow), producing new bone layer at the implant surface; osteoblasts OSC and preosteocytes are seen in woven bone WB of primary sheath bone. (C) Large magnification at white aster marked in (A) demonstrates WB including HSC, OSC, osteoblasts and osteocytes and intruding into interspace of fatty marrow.

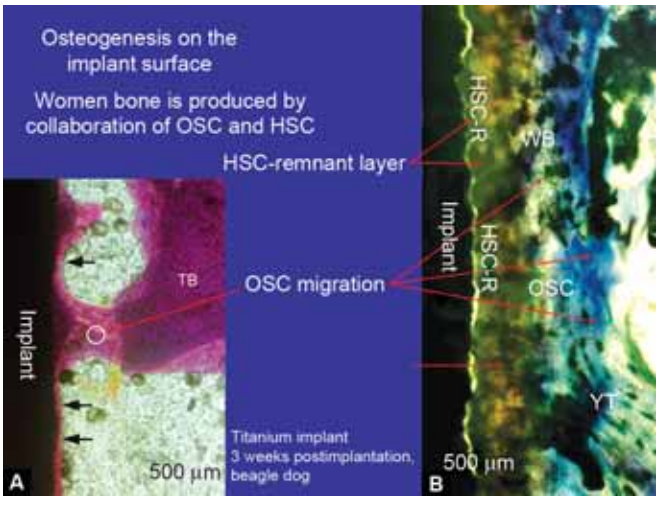

Figs 7A and B: (A) Implant surface covered by OSC migration of endosteum envelop (round mark) from drill cut edge of adjacent trabeular bone TB, three weeks postimplantation of LR (large roughness, Ra 2.0 µm). (B) OSC migration making young trabecular bone YT covers HSC or HSC-remnant layer HSC-R adhered prior to the implant surface and produces woven bone WB of primary sheath bone with collaboration of HSC at the implant surface. Separation between implant and HSC-R layer is caused by tissue shrinkage during operation of histological specimen.

Six weeks postimplantation, the woven bone apposed onto pseudo bone layer which changed from fibrous capsule to solution-mediated calcification. The pseudo bone layer was covered with multiple cell layer including mesenclymal cell and OSC migrated from endosteum of cortical bone mainly and scaresely trabecular bone envelope. The multiple cell layer could generate the new woven bone with cooperation of OSC and HSC on the pseudo bone, that is the primary sheath bone (Figs 8A and B).

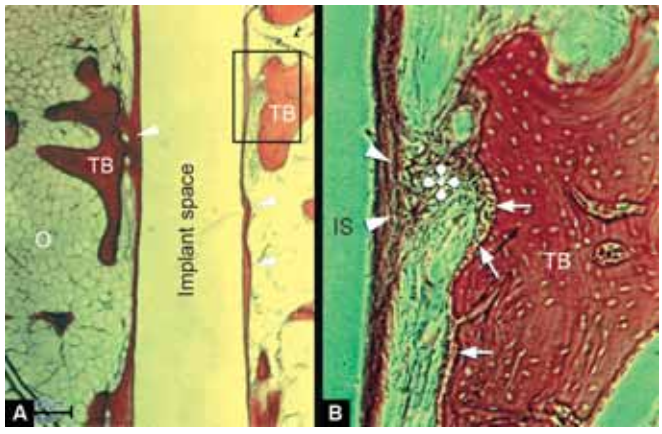

Figs 8A and B: (A) Primary sheath bone originates on the implant surface with OSC migration from endosteum-envelop of trabecular bone through yellow marrow of fatty tissue (round mark) six weeks postimplantation. (B) Large magnification of right upper square of (A) demonstrates origination of primary sheath bone at the implant surface with OSC migration to the implant surface from endosteum-envelop of trabecular bone. IS: implant space, *: OSC migration, TB: trabecular bone, arrow head: primary sheath bone, arrow: osteoblasts.

Electron Microscopic Investigation on the Formation of Primary Sheath Bone

Preosteocytes and osteocytes were buried in calcified collagen fibers layer of primary sheath bone. Osteoblasts were oriented parallel to longitudinal direction of the collagen fibers layer attending their extracellular matrix of 10-20 µm thickness six weeks postimplantation (Figs 9A and B). The cytoplasmic processes of osteoblasts extended into the extracellular matrix and collagen fibers layer and developed mineralization of the collagen fibers layer to grow new woven bone of the primary sheath bone (Figs 10A to C). As time proceeds HSC remnants including OMC was calcified by solution-mediated calcification and changed to pseudo-bone layer, which combined seamlessly to the primary sheath bone produced by cell-mediated calcification of osteoblast (Figs 11A to C).

Electron Probe Microanalysis and X-ray Diffraction

Electron probe microanalysis demonstrated calcium deposition with low density of phosphorus on the pseudo-one of solution-mediated calcification layer SMCL. The X-ray diffraction spectra indicated an amorphous pattern, unlike the crystalline structure of hydroxyapatite in true bone of cell (osteoblast)-mediated calcification layer (CMCL).

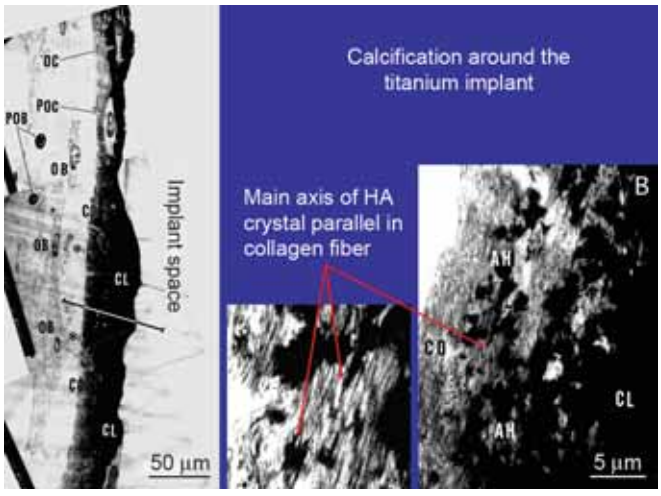

Figs 9A and B: (A) Calcificaction process of primary sheath bone. Osteocyte OC and preosteocyte POC invested in calcified layer CL and collagen fibers layer CO, osteoblast OB lineup in parallel with the collagen fibers layer, followed by preosteoblasts POB or OSC outside of OB lineup, six weeks postimplantation of LR. (B) Large mignification of * area in (A), globular deposition of hydroxyapatite and the crystal axes of allied hydroxyapatite AH coincide with longitudinal axes of CO.

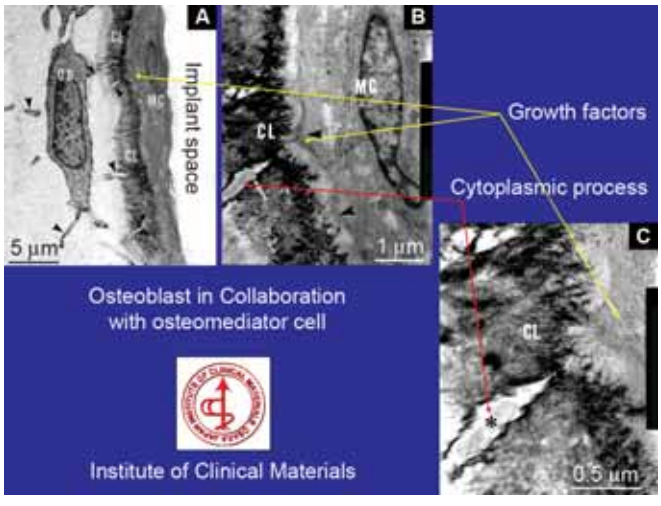

Figs 10A to C: (A) TEM demonstrates osteomediator cell MC between calcified layer CL and implant surface, MC contacts to the implant surface with electron dense membrane of 20 to 100 nm thickness. Osteoblast OB mediated by MC produces CL with hydroxyapatite deposition from matrix vesicles, which released from the cytoplasmic processes of OB (arrow head) six weeks postimplantation (see Figure 11(A)). (B) Large magnification of MC in (A). MC takes slender shape, flattened nucleus and enlarged ER. Cytoplasmic protrusions (arrow head) are releasing electron dense particles of growth factor to vicinity of osteoblastic process (arrow). Hydroxyapatite (HA) deposition demonstrates orientation of early calcified layer CL. (C) Large magnification of (B), electron-dense particles (yellow arrow) disperse toward osteoblastic process (*) through CL, needle-shape HA crystal deposition into microfibrils of collagen.

Electron probe analysis of calcium and phosphorus in SMCL demonstrated the presence of phosphorus-deficient calcified layer with 5 to 40 µm thickness of Ca/P ratio 4.17, compared with Ca/P ratio 1.5 to 1.7 in true bone, CMCL

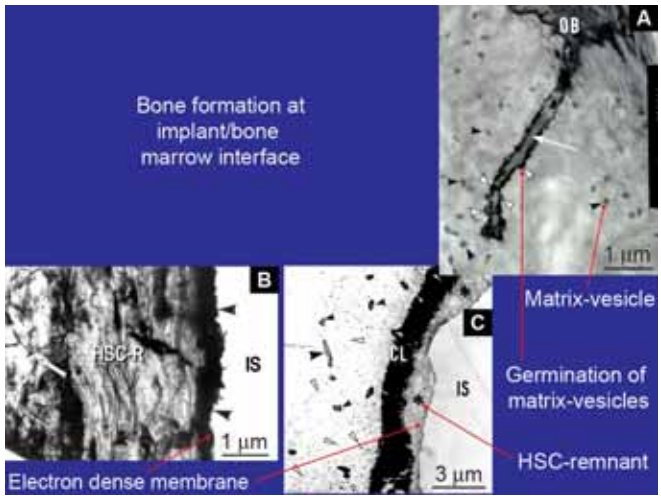

Figs 11A to C: (A) Large magnification of cytoplasmic process of osteoblast OB in bottom part of Figure 10(A), a number of matrix-vesicles (black arrow heads) and functional germinations matrix-vesicles (white arrow heads) on the unitmembrane of the cytoplasmic process (white arrow). (B) Degenerated cell-organella in HSC-R adhered to the implant surface with electrodense membrane (arrow heads), HA crystals (arrow) in the beginning of calcification by osteoblast mediated with MC, three weeks postimplantation of LR. (C) TEM demonstrates cellular remnants of HSC (*) including platelets and monocytes between CL and implant surface and HSC-R contacting to the implant surface with 20 to 100 nm thick electrodense membrane, three weeks postimplantation of LR.

(Figs 12A to C).[10] As the time proceeds SMCL developed the calcification. HSC and OMC were buried in the pseudo-bone layer of SMCL. The primary sheath bone originated from the surface of pseudo-bone layer. Therefore, OMC and HSC were hardly seen at the implant/bone interface six weeks postimplantation, due to completion of Ca deposition with SMCL at the interface. Osteoblasts were arranged in parallel to the implant surface with extracellular matrix and intervenient layers consisted of collagen fibres layer, CMCL and SMCL (Fig. 9A). Direct deposition of mineralized tissue, SMCL and CMCL to the implant surface appears to be an inevitable phenomenon in bone tissue, similar to connective tissue encapsulation of foreign body reaction in soft tissue. Successively, the woven bone layer of the primary sheath bone was apposed with lamellar bone and developed to mature sheath bone as a supporting structure of implant.

Maturation of Primary Sheath Bone

The primary sheath bone was restructured by apposition of lamellar bone with typical osteoblastic layer, and primary osteons were observed parallel to the implant surface circularly and vertically. The reconstructed primary sheath bone demonstrated a complicated implant supporting structure 24 weeks postimplantation. The lamellar bone apposition was controlled by bone resorption and formation

according to magnitude and frequency of strains in the primary sheath bone under functional biting load. Then the primary sheath bone changed to mature sheath bone, 24 to 54 weeks or more postimplantation. Compact lamellar bone developed actively under the biting load and the mechanical strength of the sheath bone was reinforced with complicated structure of the lamellar and mature bone (Figs 13A and B).[7]

Close Relation between Healing Process and Endosteum

These histological investigations certified that the sheath bone formation was closely related to existence of endosteum at the implant surface in bone marrow. The healing process in the early stage may be strongly controlled with endosteum and periosteum, therefore the process is delayed more with longer distance from the endosteum of cortical bone to the implant surface. It is revealed that the sheath bone formation depends upon mainly breadth of implant/cortical bone interspace and arrival time of OSC migration from endosteum to the implant surface. Unfortunately, this study could not clarify the topographic dependency on the sheath bone formation between SR of Ra 0.4 ± 0.01 μm and LR of Ra 2.0 ± 0.12 μm (Table 1).[7]

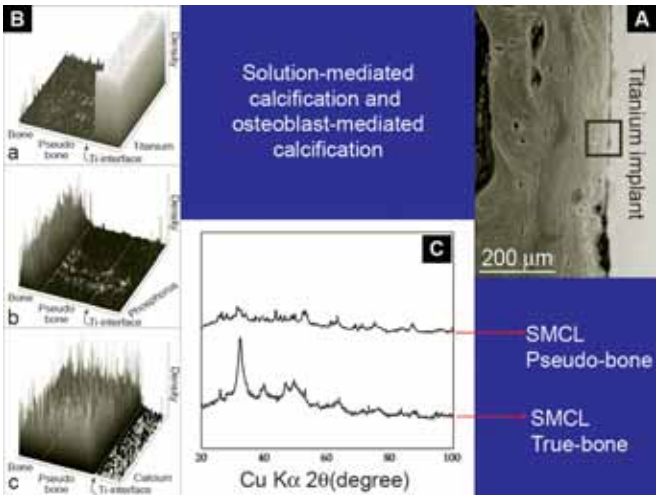

Figs 12A to C: (A) SEM of the sheath bone surrounding titanium implant. (B) Electron probe microanalysis on the titanium implant and bone marrow interface in 100 x 100 μm square in (A), a: Titanium detection, b: Phosphorus, c: Calcium, Ti: Titanium implant, Pseudo-bone: solution-mediated calcification layer, Bone: osteoblast-mediated calcification layer. (C) X-ray diffraction patterns at the true bone layer (lower) and pseudo bone (upper)

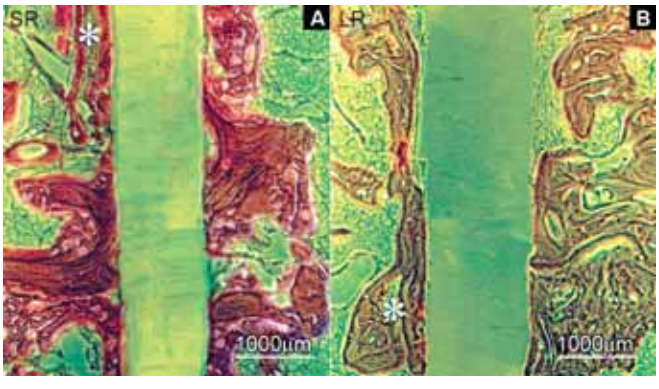

Figs 13A and B: (A) The sheath bone covers implant surface and represents turnover phenomenon of bone formation/resorption at the implant/bone interface according to the magnitude and number of biting load. Implant: SR, 24 weeks postimplantation. (B) Cone-shaped resorption of crestal bone loss occurs at the neck of implant, where most of the stress concentration is generated, while close bone contact has been kept at the deep and apical area. Implant: LR, 24 weeks postimplantation

Table 1: Sheath bone contact to titanium implant

Implant	*Surface roughness (μg)*	*Bone Contact (%)*	
		6 weeks	*24 weeks*
BP	Mirror-like	22.4 ± 9.96	74.9 + 10.94
SR	Ra 0.4 ± 0.01	26.4 ± 8.29	69.8 ± 9.04
LR	CB • 4HF120		
	Ra 2.0 ± 0.12	33.4 ± 7.44	66.6 ± 11.02

BP: Barrael polish, SR: Small roughness, CB: Corrundum blasting, 4HF60 sec and 4HF-8H_2O_2 15 sec, LR: 4HF120: Corundum basting and 4HF 120 sec + 4F – 8H_2O_2 15 sec, six weeks: Young bone contact (linear %) 24 weeks: bone contact (linear %) ±: Sample standard deviation, n = 5.

SHEATH BONE FORMATION IN CERAMIC IMPLANT

Extensive progress in ceramic technology has led to the discovery of a variety of materials whose chemical, physical and mechanical properties confer a high degree of stability, bioactivity and osteoconductivity. This makes them suitable candidates for long-term implants within living tissue. The stable ceramics, such as alumina, zirconia, silicon nitride, vitreous carbon, and nano-grained hydroxyapatite and high toughness ceramic composites (alumina, zirconia, yttria, etc.) have been developed for dental implants. In 1975, single crystal alumina of sapphire and polycrystal alumina composite containing ZrO_2, Y_2O_3, $BaCO_3$, T_2O_3, TiO_2, etc., which was named by Bioceram® and in market for 20 years. They have high survival rates of 92.65 ± 8.40% as reported in recent year (Fig. 14)[11-13] and 3 mol% Y_2O_3-zirconia has been spotlighted as a single stage implant nowadays. In this paper, the sheath bone formation around the ceramic implant will be explained by histometric measurement in animal experiment to understand the successful condition of the ceramic implant under the immediate loading.

MATERIALS AND METHODS

Six months after extraction of M_1, M_2 in the both side of jaw bones of four monkeys, *Macaca fascicularis*. About

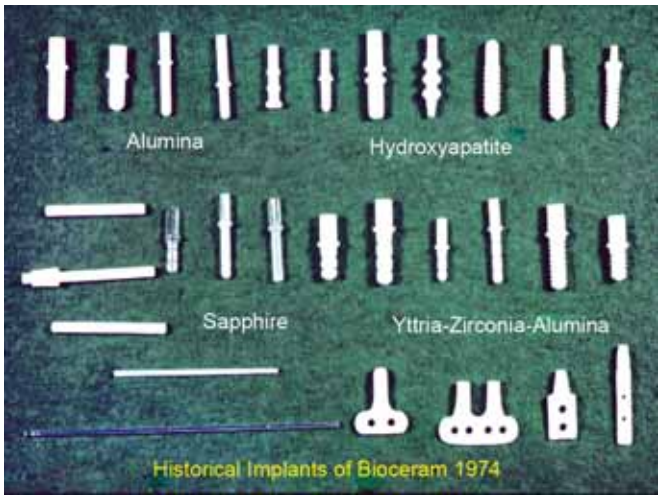

Fig. 14: Bioceram implants made of alumina polycrystal and single crystal sapphire, dense hydroxyapatite and yttria-zirconia-alumina composite, 1973 to 1980.

37 implants of Bioceram® were implanted into monkey mandible. Each two implants were installed into the right side and connected with metallic bridge of P_2 and M_3 to oppose biting stress one week postimplantation (Fig. 15).[14] Other two implants were installed into the left side and protected from the biting stress with metallic bar bridge between P_2 and M_3, as a control group of unload. After removing the implants, the bone tissue blocks were sectioned in mediodistal direction with 20 µm thickness and stained with H and E and Azan-Mallroy. Bone contact (linear percent) to the implant surface and bone occupancy (area percent) within 500 µm limits surrounding the implant were measured by a histometry with NIH image version 1.61 connected to a Mac G4, on phase contrast micrographs. The measurement was limited within 3 mm length of the implant root in bone marrow, corresponding to 1 mm away from endosteal edge of crestal bone because sheath bone growth rate at the implant surface was influenced with distance from the endosteal edge of crestal bone (See, close relation between healing process and endosteum).

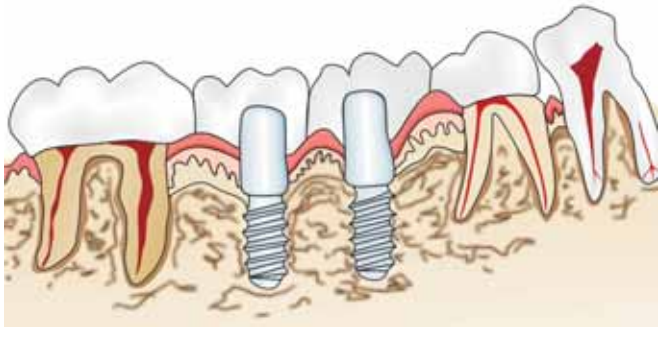

Fig. 15: Ceramic implants were fixed with less than 50 µm of micromotion in monkey's mandible by combining to the proximal teeth of P2 and M3 with metallic bridge of Au-Pd-Ag alloy.

Sheath Bone Formation

Bone chips cut off by drilling were observed in mesenchymal like tissue between the implant threads one week postimplantation. Woven bone growth on the implant surface developed to primary sheath bone significantly grew from 2 to 4 weeks postimplantation (Figs 16A and B). The primary sheath bone increased in thickness with lamellar bone apposition from 4 to 16 weeks postimplantation and developed in the sheath bone. Thicker sheath bone was produced in the case of loaded implants than unloaded implants 8 to 16 weeks postimplantation (12 to 24 weeks postimplantation in human) (Figs 17A and B).[14,15]

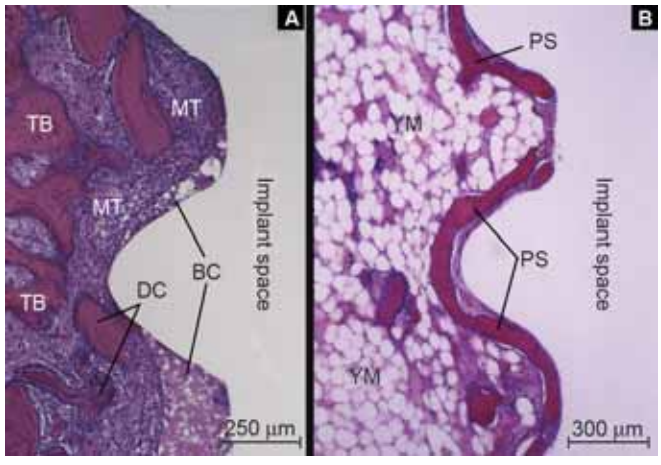

Figs 16A and B: Origination of primary sheath bone in the ceramic implant. (A) One week postimplantation, the implant surface is covered with blood clot BC, depressed by granulation of mesenchymal tissue MT including drill-cut bone chips. (B) 12 weeks postimplantation, the implant surface is covered with primary sheath bone PS of woven bone. TB: trabecular bone, DC: drill-cut bone chip, MT: mesenchymal tissue, PS: primary sheath bone, YM: yellow marrow

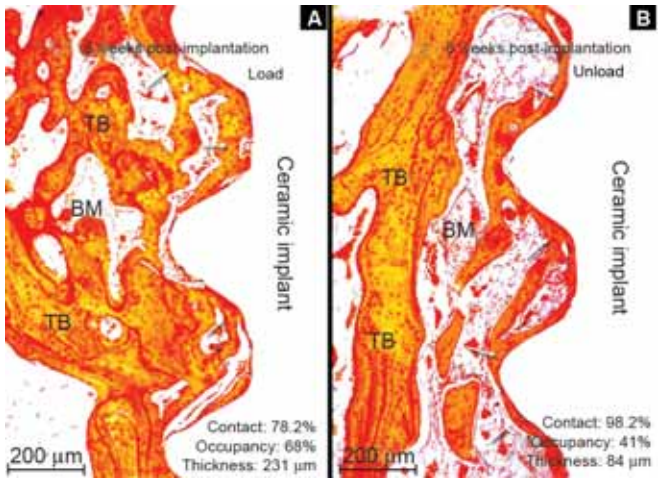

Figs 17A and B: Bone contact and occupancy in ceramic implant, eight weeks post implantation. (A) The implant surface is lined with thicker sheath bone under functional loading compared with that of (B) unloading. Arrow: implant sheath bone, TB: trabecular bone, BM: bone marrow (*Courtesy:* Dr T Sugimoto).

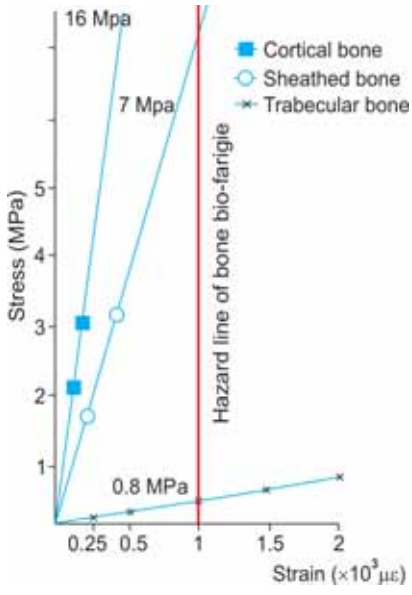

Fig. 18: Stress and strain of cortical, sheathed and trabecular bone. Compressive strength and elastic modulus: Cortical bone 100 MPa and 15 GPa, sheathed bone 50 MPa and 7 GPa, trabecular bone 8 MPa and 0.3 GPa. Compressive strength for 1000 microstrain of bio-fatigue: Cortical bone 16 MPa, sheath bone 7 MPa. Numerical values were estimated from data book on mechanical properties of living cells, tissues and organs 1996, H Abe, K Hayashi and M Sato (Eds), Springer-verlag, Tokyo

Bone contact length (mm) and thickness (μm) of the sheath bone increased from 10.9 mm and 350 μm, Four weeks postimplantation to 12.8 mm and 410 μm, 16 weeks postimplantation under the functional biting load. It was noticeable result that the sheath bone became to be thicker under the functional biting load than unloaded sheath bone at the 16 weeks postimplantation, inspite of no significant difference between the both bone contacts of loaded implant and unloaded (Table 2). From these findings, it is estimated roughly that the sheath bone under the functional load of 100N may cause compressive stress 68 MPa, four weeks post-implantation and 19 MPa, 16 weeks postimplantation. These stresses (MPa) may cause over 1000 με of biological fatigue in the sheath bone (Fig. 18 and Table 3). As a result investigating these data, it is revealed that maintenance of the sheath bone requires one of following four conditions to resist functional biting stress until four months (six months in human) after the implantation:

1. Sufficient anchor between implant and cortical bone
2. Implant fixation with metallic stent on alveolar bone
3. Fixation by connection with approximal steady implant and/or healthy tooth
4. Nonload bearing (submersible implant).

24 to 52 weeks postimplantation, the sheath bone developed more lamellar bone apposition and maturation with passage of time. However, bone formation and resorption of remodeling cycle continued at the implant/bone interface under the functional biting load during the entire lifetime of the implant, and this process seems to be crucial for the maintenance of implant fixation, exposed to variable biting load.

SHEATH BONE RESPONSES TO MICROMOTION

There is no consensus on load-free time between implant installation and prosthetic restoration. So far, 20 weeks or more postimplantation were required to obtain reliable fixation of implant with sufficient bone contact and thickness of the sheath bone, as well as anchorage at the implant/bone interface with micro- and macro-levels.[16] This period was founded by clinical studies to be optimal for bone to adapt to the new biomechanical conditions created by both surgery and the presence of a titanium implant, as reported by D Chappard et al.[17] Loading an implant too early would induce increased microstrains responsible for micromotions, which would lead to formation of a fibrous tissue at implant/bone interface.[18]

How to Control Micromotion?

Implant specialist has responsibility to minimize over load of 8 MPa (1000 με) on the sheath bone that bears occlusal load through the superstructure of implant.[6] From the animal

Table 3: Bone fracture and minimum effective strain

Bone fracture	
Fracture	> 8000 με
Mechanical fatigue	2000-3000 με
Biological fatigue	1000-2000 με
MES of bone modeling and remodeling	100-1000 με

Table 2: Sheath bone contact and thickness

Loading term and load/unload	*4 weeks*		*8 weeks*		*16 weeks*	
	Load	*Unload*	*Load*	*Unload*	*Load*	*Unload*
Bone contact (mm)	10.9 ± 9.4	10.2 ± 4.0	11.7 ± 4.0	13.2 ± 4.2	12.8 ± 5.5	14.5 ± 4.0
Bone thickness (μm)	135 ± 45	90 ± 90	335 ± 90	700 ± 75	410 ± 50	290 ± 55

N = 5, ±: Sample standard deviation
Two failure implants were rejected from this statistic.

experiments, it is estimated that the early loading increases micromotion and gives rise to microstrain of 1000 με or more (biological fatigue, Fig. 18) in the sheath bone, due to immaturity of lamellar bone apposition and compaction to the sheath bone within 16 weeks postimplantation (24 weeks in human). If the implants are protected from micromotion during functional biting load by satisfying one of four requirements (see sheath bone formation), the sheath bone can increase the thickness and maturation by lamellar bone apposition and compaction under the early load. As a result the implant is successfully fixed to the surrounding bone.

How to Read Micromotion Numerically?

According to the reports of Brunski et al,[19,20] the rule of thumb is that relative motion of more than 100 μm should be avoided for the construction of osseointegration. But the 100 μm is not an exact definition with clinical evidence but data of computer simulation. We proved that the sheath bone formation could develop and perform at the implant/bone interspace with limited micromotion of less than 50 μm under the condition of immediate loading. The 50 μm was computed from animal experiments and clinical examinations on the relationship between displacement of implant and the Periotest® value (PTV) (Fig. 19). The animal and clinical experiments represented the possibility of digital reading on the micromotion of implant with the PTV, that might indicate digitally the micromotion of the implants and teeth under functional biting load. The histometric investigation demonstrated that the sheath bone growth developed at the implant surface under the condition of immediate loading and particularly increased bone contact and thickness of the sheath bone from 6 to 24 weeks postimplantation (Table 1). The teeth, P_2 and M_1 supported two implants indicated PTV 0.5 to 5.7, corresponded to micromotion 10 to 50 μm estimated from the PTV. From these findings, it is revealed that implant supported by metallic bridge with healthy tooth may grow the sheath bone under the functional loading (see Figs 7 to 9). More clear-cut evidence of the sheath bone formation around the implant with micromotion of natural tooth was recognized with osteogenesis and osseointegration around the endodontic pin stabilizer under the functional biting load inspite of material difference, Al_2O_3, Co-Cr-Mo and titanium (Figs 20 and 21).[6,21] No evidence of topographic dependency on bone formation around implant was confirmed[7] and the immediate loading is successful procedure in every implant made of different biomaterials, designs and surface topographies, when the steady stability within 50 μm of micromotion is achieved and kept through out the implant life.[22]

Fig. 20: Two pin stabilizers were inserted into M_1 of beagle's mandible and fixed with Fuji IX of glass ionomer cement

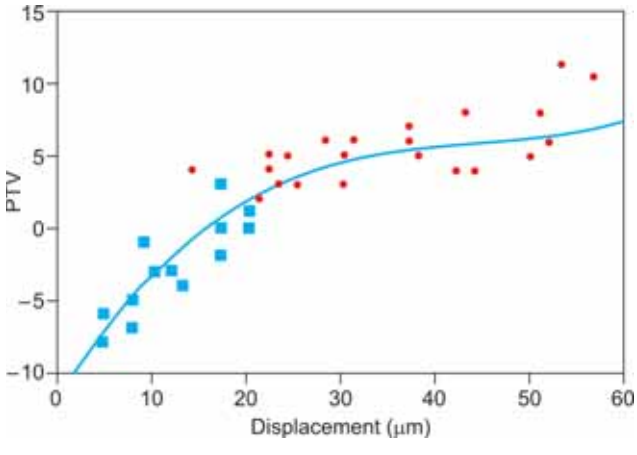

Fig. 19: Horizontal displacement (μm) of 22 incisors (PTV + 3 ± 11) and 13 screw type implants (PTV –7 ± 3). Three years or more post implantaion were measured by noncontact sensor under the horizontal loading of 8 N, 10 seconds and compared with each PTVs. ■: implant, ●: natural teeth, 11 and 21[6]

Co-Cr-Mo, Al_2O_3

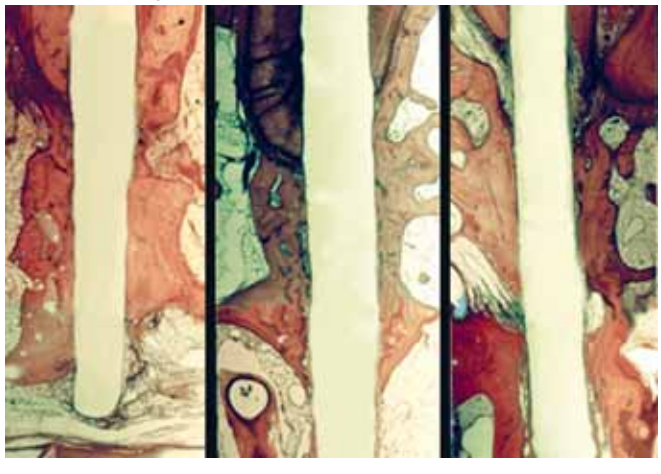

Fig. 21: Matured sheath bone around the endodontic pin stabilizer made of commercially pure titanium, Co-Cr-Mo alloy and single crystal alumina, 24 weeks postinsertion. Star mark: root apex, YM: yellow marrow, SB: sheath bone

These animal experiments demonstrated that the implant could develop osteogenesis and perform osseointegration under the condition of immediate loading because the implant was controlled within 50 µm of micromotion, detected with PTV ≤ +5. It is revealed that the connection of implant to adjacent healthy tooth is useful method to control the micromotion until completion of the sheath bone maturation. However, it will be better to release the connection after the sheath bone maturation.

How to Evade Biting Impact for Sheath Bone Formation?

It is a natural process to cause occlusal disharmony in occlusal scheme reconstructed with natural tooth and implants, because of large difference of elastic modulus between natural tooth with 1.115 ± 0.239 MPa of periodontal ligament and implant with 9.2 to 16.7 GPa of implant-bone interface.[23,24] The occlusal disharmony should be adjusted to function in harmony with rest of the stomatognathic system.

On the adjusting procedure for the occlusal disharmony during mastication, CE Misch and MW Bidez[25] have reported that depression of implant position with thin articulating paper (less than 25 µm thickness) was effective for the initial implant occlusal adjustment in centric occlusion under a light tapping force, that was expressed mathematically with 23 µm difference of intrusive movement between natural tooth (28 µm) and implant (5 µm) under the light biting force. The implant prosthesis should barely contact, and the adjacent teeth should exhibit greater initial contact. Hence to harmonize the occlusal forces between implants and teeth, a heavy bite force occlusal adjustment is used because it depresses the natural teeth, positioning them closer to the depressed implant position and equally sharing the load. On the anterior teeth, exhibits greater discrepancies in lateral movement compared with posterior implant. The occlusal adjustment in this direction is more critical to implant success and survival. Light force and thin articulating paper are first used to ensure that no implant crown contact occurs during the initial movement of the teeth.

50 µm laterally (anterior) and 23 µm vertically (posterior) depression on implant position might be decided based on initial movements under 20 N of biting load.[26] However, it is very difficult to decide the size of depression in implant position due to various patterns of biting impact in each clinical case. Then, we have recommended ICM's adjusting procedure that is about 50 µm depression of roughly large scale compared with mathematical discrepancy of 23 µm reported by CE Misch.[25] About 50 µm of discrepancy between the both initial movement of implant and natural tooth is able to be adjusted easily by grinding with abrasive point and/or powder. The 50 µm was decided from the two reports on elastic displacement of natural teeth under vertical load of functional biting, demonstrated average 37 µm, 22 to 42 µm[27] and average 50 µm, 30 to 58 µm under 8 N vertical load (unpublished data in ICM). Natural tooth opposing to implant has a travelling behavior of free displacement in alveolar bone according to the form of clearance between the both occlusal surface of implant and the opposed tooth. Natural teeth have embryological behavior on the displacement, i.e. extrude, rotate and migrate in alveolar bone, caused by external light forces from tongue, baccalis, occlusal load, etc. to make effective and functional occlusion. On the contrary, the fixed implant does not exhibit any displacement in alveolar bone even under powerful occlusal load, while the alveolar bone and jaw bone changed not only endosteal structure but also external form.[28] In the case of implant opposing to implant, a strict occlusal adjustment is required to make suitable occlusal condition in the location and direction of implant's axis in maxillomandibular bone, because it is an effective trigger to reconstruct the suitable stomatognathic mastication system.

Biodynamic Interface

Bone is maintained by the modeling and remodeling which is load dependent. The amount of bone formation per unit time (Vf) and the amount of bone resorption per unit time (Vt) were obtained from a histometric investigation of bone double-labeled with tetracycline.[29,30] Using these parameter, the change in the amount of bone per sectional area fraction (Δ Afract) can be defined by the following equation.

$$\Delta \text{ Afract} = Vf - Vt$$

±Δ Afract mean increasing of implant loosening (–) or fixation (+).

Animal examinations and clinical investigations on wound healing of bone modeling and remodeling after implant surgery have been carried out by many researchers, mentioned above. In many of these studies, a multitude of shapes, sizes, materials, and animal models has precluded any generally accepted rules for "favorable/unfavorable" interfacial stress transfer conditions, as reported in the review papers of Brunski.[18-20] As one approach to the favorable condition, a mathematical analysis on bone resorption and formation of mechano-sensitive bone tissue under the repeating load was carried out by Morita.[31] He investigated the influence of mechanical stimulation on self-healing behavior of bone in relation to fatigue life of living bone. The histometric analysis was carried out by measuring

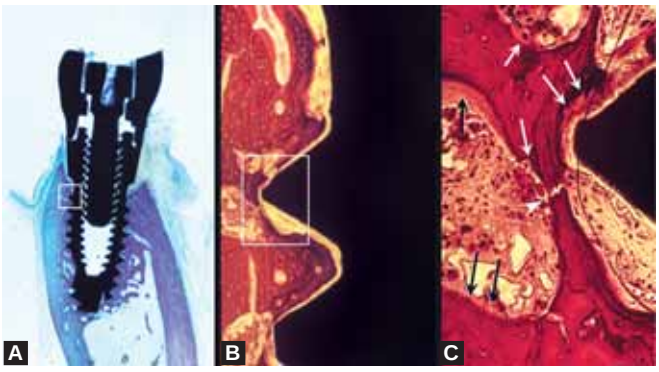

Figs 22A to C: Biodynamic response of the sheath bone to functional load for two years and half. (A) Implant has been supported with cortical bone and the sheath bone has covered completely the implant root. (B) Magnification of square region in (A). (C) Large magnification of square region in (B) demonstrates three different view of bone fracture (arrow head), resorption (white arrow) and formation (black arrow) around the first thread. Magnification: 357 µm/mm (A), 30 µm/mm (B), 16.5 µm/mm (C)

the accumulation rate of bone damage caused by cyclic loadings and its remodeling activities at the rest time after the loading. The fatigue life of living bone was formulated as follows:

$$T = 1/\{f/N - (V_f/V_0)/t_0\}$$

where

T = fatigue life of living bone
f = frequency of cyclic load
N = repeating number of cyclic load
V_f = volume of new bone formation/cm^3
V_0 = volume of original bone/cm^3
t_0 = testing time.

Bone resorption and formation should be observed constantly in alveolar bone under functional biting stress. The resorption area is restored with soft tissue including osteogenic cells and may have a buffering effect to the biting impact during mastication. If the implant is kept within 50 µm micromotion, the soft tissue may change to sheath bone. Long-term histological observations demonstrated that implants were supported with a biodynamic interface, which represented both the status of bone resorption and formation occurring simultaneously at different sites of the implant/bone interface and a turnover phenomenon of bone formation and resorption at the same site 12 weeks interval in dog (18 weeks in human). To explain functional fixation of the implant, hypothesis of fibro-osseous integration has been suggested by Weiss.[32] However, the attempt to create a peri-implantium is apt to introduce loosening of the implant, because of the difficulty of maintaining favorable thickness of the peri-implantium for successful conditions of a implant. It is difficult to investigate the true nature of long-term interactions at the implant-bone interface under functional condition from the data of pinpoint observations on limited area and time by light and electron microscopy. It is important to collate the both data from basic research and clinical investigation for long-term throughout the implant life. The implant-bone interface is a biodynamic interface[33] with turnover phenomenon, bone resorption and formation of remodeling cycle with 18 weeks interval in human. The healthy condition of implant is to be controlled by self healing behavior of living bone (Figs 22A to C). Further studies on the biodynamic interface are needed to increase reliability of dental implant fixation.

The author would like to thank Ms. M Kamatani, her helpful assistance for preparing the manuscript of this review paper and Dr T Sugimoto, his kind cooperation to animal experiments.

REFERENCES

1. Kawahara H. Difficulty of biological standardization for biomaterials. Tissue Culture in Dentistry 1982;19:39-43.
2. Mjor IA, Hensten-Petterson A, Skogedal O. Biologic evaluation of filling materials, a comparison of results using cell culture technique, implantation test and pulp studies. Inter Dent J 1977;27:124-29.
3. Klötzer WT. Personal communication 1980.
4. Kawahara H, Imai K, Kawahara D. Photo-pattern analysis and computation in the evaluation of the cytotoxicity of dental materials in vitro. Inter Endo Jour 1988;21:100-05.
5. Ratner BD. On the ubiquity of the healing reaction. Titanium in Medicine. Branette DM, Tengvall P, Textor M, Thomsen P (Eds). Berlin springer 2001:7-9.
6. Kawahara H, Kawahara D, Hayakawa M, Tamai Y, Kuremoto T, Matsuda S. Ossseointegration under immediate loading; Biomechanical stress-strain and bone formation-resorption. Implant Dent 2003;12(1):61-66.
7. Kawahara H, Aoki H, Soeda Y, Kawahara D, Matsuda S. No evidence to indicate topographic dependency on bone formation around commercially pure titanium implants under masticatory loading. JMSM 2006;17:727-34.
8. Niwa K, Kawahara D, Ii K, Nakamura T, Kawahara H. Statistical analysis on the region-difference of alveolar bone density. Proceedings of 5th WCOI 2001;190-91.
9. Kawahara H, Soeda Y, Niwa K, Takahashi M, Kawahara D, Araki N. In vitro study on bone formation and surface topography from the standpoint of biomechanics. JMSM 2004; 15:1297-307.
10. Kawahara H, Nakakita S, Ito M, Niwa K, Kawahara D, Matsuda S. Electron microscopic investigation on the osteogenesis at titanium implant/bone marrow interface under masticatory loading. JMSM 2006;17:717-26.
11. Kawahara H. Bioceramics for hard tissue replacements. Clinical Material 1987;2:181-206.
12. Steflid DE, Koth DL, Rovinson FG, McKinney RV, Davis BC, Morris CF, Davis QB. Prospective investigation of the single-crystal sapphire endosteal dental implant in humans: Ten-year result. J Oral Implant 1995;21:8-13.
13. Kawahara H, Hirabayashi M, Hamano Y. Burnt ceramic bone implant, 90–50% of Al_2O_3, ZrO_2, La_2O_3 and Y_2O_3. US Patent 1979;4155124:1-3.
14. Toshimori H, Soeda Y, Takayasu Y, Nakanishi K, Hayakawa M, Sugimoto T, Kawahara D. Bone contact and bone occupancy

around single stage implant loaded and unloaded. Jour Oromax Biomech 2006;12(1):37-40.
15. Piattelli A, Corigliano M, Scarano A. Microscopical observations of the osseous responses in early loaded human titanium implants: A report of two cases. Biomaterials 1996;17(1):333-37.
16. Brånemark PI. Introduction to osseointegration. Brånemark PI, Zarb GA, Albrektsson T (Eds). Tissue-integrated prostheses: Osseointegration in clinical dentistry. Chicago: Quintessence; 1985:11-76.
17. Chappard D, Aguado E, Huré G, Grizon F, Basle MF. The early remodeling phases around titanium implants: A histomorphometric assessment of bone quality in a 3- and 6-month study in sheep. JOMI 1999;14:189-96.
18. Brunski JB, Moccia AF, Pollack SR, Korostoff E, Trachtenberg DI. The influence of functional use of endosseous dental implants on the tissue-implant interface I. Histological Aspects. J Dent Res 1979;58(10):1953-69.
19. Brunski JB, Pules DA, Nanci A. Biomaterials and biomechanics of oral and maxillofacial implants: Current status and future developments. JOMI 2000;15:15-46.
20. Brunski JB. Biomechanical factors affecting the bone-dental implant interface. Clinical Materials 1992;10:153-201.
21. Matusda T, Mimura Y, Niwa K, Kawahara H. Study on the osteogenesis and osseointegration around the endodontic pin implant, in relation to immediate loading. Proceedings of 5th WCOI 2001;116-17.
22. Neugebauer J, Weinlander M, Lekovic V, Berg KHL, Zoeller JE. Mechanical stability of immediately loaded implants with various surfaces and designs: A pilot study in dogs. IJOMI 2009; 24:1083-92.
23. Nishihira M, Satoh Y, Morikawa H, Yamamoto K, Ishikawa H, Nakamura S. Measurement of compressive elasticity of periodontal ligament. J Oromax 1996;2(1):31-32.
24. Komatsu K, Chiba M. The effect of velocity of loading on the biomechanical responses of the periodontal ligament in transverse sections of the rat molar in vitro. Archs oral Biol 1993;38(5):369-75.
25. Misch CE, Bidez NW. Occlusal consideration for implant-supported prosthesis: Implant protective occlusion and occlusal materials. Contemporary implant dentistry. Misch CE. St. Lous (Eds). Mosby; 1999:609-28.
26. Sekine H, Komiyama Y, Hotta H, Yoshida K. Mobility characteristics and tactile sensitivity of osseointegrated fixture-supporting system. Tissue integration in oral and maxillo-facial reconstruction. Von Steenberghe Amsterdam D (Eds). Excerpta Medica 1985:326-32.
27. Kishimoto Y. The creap of periodontal ligament. J Prost Dent 1981;22(1):154-66.
28. Roberts WE, Smith RK, Zirberman Y, Mozsary PG, Smith RS. Osseous adaptation to continuous loading of rigid endosseous implants. Am J Orthod 1985;86(2):95-111.
29. Morita M, Itoman M, Yamamoto M, Sasada T. The influence of mechanical stimulation on the self-healing behavior of cancellous bone part 1. Measurement of remodeling activity depending on a cyclic loading. JJSB 1986;4(2):77-85.
30. Morita M, Sasada T, Itoman M, Yamamoto M. The influence of mechanical stimulation on the self-healing behavior of cancellous bone. Part 2 in vivo fatigue properties of bone. JJSB 1986; 4(4): 175-81.
31. Morita M. Fatigue life of live bone, in oral implantology. Kawahara H (Eds). Tokyo; Ishiyaku Pub 1991:75-90.
32. Weiss CM. Tissue integration of dental endosseous implants—description and comparative analysis of the fibroossseous integration system. J Oral Implantol 1986;12:169-214.
33. Kawahara H. Biodynamic interface. Biomaterials for dental implants. Wise DL, Trantolo DJ, Altobelli DE, Yaszemski MJ, Gresser JD, Schwartz ER (Eds). NY: Marcel Dekker Inc 1995:1514-15.

Haruyuki Kawahara
e-mail: office@icm.ac